Experimental and numerical study of behaviour, damage and crack propagation of PA6

Cédric Regrain[1,a], Lucien Laiarinandrasana[1,b] and Sophie Toillon[2,c]

[1]Centre des Matériaux – Ecole Nationale Supérieure des Mines de Paris – UMR CNRS 7633

BP 87 – F 91003 Evry Cedex – France

[2]LAMPC – BP 82617 – 44326 Nantes Cedex 03 – France

[a]cedric.regrain@ensmp.fr, [b]lucien.laiarinandrasana@ensmp.fr, [c]sophie.toillon@cetim.fr

Abstract

Polyamide 6 (PA6) is a semi-crystalline polymer utilised in many structural components working under steady load. At room temperature, PA6 exhibits time dependent (viscoplastic) deformation. The aim of this work is to investigate the PA6 mechanical response and the crack growth under creep conditions.

The experimental database consists of tests carried out on smooth, notched and cracked round bars. Load versus displacement curves were recorded for tensile monotonic tests at various crosshead speeds. Then, creep tests with constant loads were performed allowing the record of the creep strain history according to the applied load.

Microscopic observations highlight the initial spherulitic structure.

Smooth, cracked and notched specimens were utilised in order to identify material coefficients dedicated for both analytical and FE modeling. The non linear fracture mechanics (NLFM) for creeping solids was applied to the cracked specimen test results. For this kind of loading, the use of the load parameter C^* is recommended. Thanks to the database, C^* values could be determined analytically for each creep crack test. A comparative study of load parameters C^* and C_s^* is performed.

By plotting C^* values versus time to failure, a unique correlation was obtained. The knowledge of this master curve allows to assess the lifetime of PA6 cracked bodies, provided that C^* parameter can be calculated.

Introduction

Nowadays, structural polymers are frequently used in engineering components subjected to thermo-mechanical loadings. To assess the durability of such components, the knowledge of the mechanical behaviour of the material is a key issue. This paper deals with Polyamide 6 (PA6) that essentially works under steady load. The creep behaviour is then addressed here. The objective for this kind of study is to access the lifetime of PA6 cracked bodies under steady load. The load parameter C^* recommended by the Non Linear Fracture Mechanics (NLFM) for this kind of loading has ever been estimated in other studies essentially for metallic material [1, 2]. The application of this parameter to polymer material seems to be relevant provided that it can be calculated.

Investigated PA6 material

The material under study is a polyamide 6 (PA6) provided by Angst & Pfister as 610mm x 1.230mm flow molded plates with 10mm thickness.

The PA6 is a semi-crystalline polymer. In order to reveal the spherulitic microstructure, samples were examined by Scanning Electron Microscopy (SEM) after chemical etching. Fig.1 shows that the spherulite mean size is about 6μm.
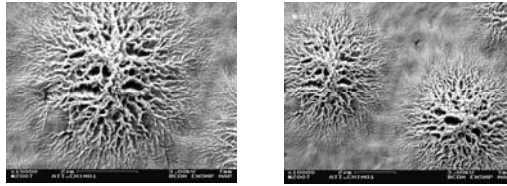

Fig.1. S.E.M. observation of the spherulitic microstructure

Essentially round bar specimens were machined from these plates (Fig.2). They were cut from the plates in three directions in order to verify the isotropy of the material.
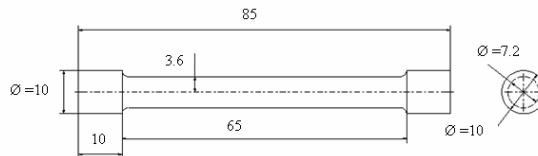

Fig.2. Scheme of the smooth specimen (ASTM D638-91 and D2990, all dimensions in mm)

Experimental procedure

Tensile and creep tests were performed on smooth, notched and cracked round bars (Fig.2) at room temperature (25°C) and under controlled humidity condition of 50%. To achieve this goal, an electromechanical test machine provided with a load cell was used. The specimens were instrumented with a laser beam device to monitor the deformation. Post-mortem SEM examinations of the fracture surfaces are systematically carried out at the end of each test.

Tensile tests

Monotonic tensile tests are essentially carried out on smooth round bars to better control the loading step for the creep tests. These tests were performed on round bars at three crosshead speeds: 100, 40 and 10mm/s. Fig.3a shows the nominal stress F/S_0 versus engineering strain $\Delta L/L_0$ plot. F/S_0 is the load divided by the initial cross section and $\Delta L/L_0$ is the variation of displacement divided by the initial gage length. It seems that a slight effect of the crosshead speed is evidenced.
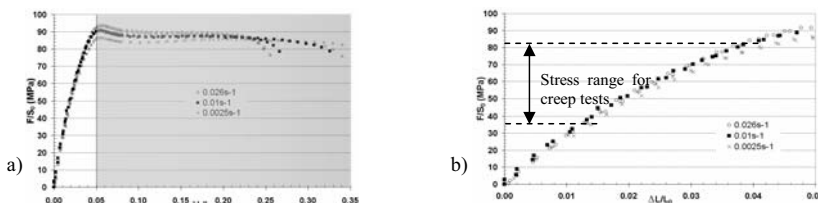

Fig.3. Stress versus Strain for tensile monotonic tests for three various crosshead speeds – a) Global curve until rupture, b) zone of interest for loading stage of creep tests

Therefore the creep tests will be performed with the maximal crosshead speed for the loading stage in order to limit this strain rate effect. Furthermore, Fig.3a allows the maximum stress for

creep tests to be defined. The value of the plateau stress (82MPa) was then selected here. Fig.3b focuses on the loading part of stress-strain curves where the stress range [36MPa-82MPa] for creep tests is indicated.

Creep tests on smooth bars

Creep tests were carried out on the same apparatus and the same specimens with the maximum crosshead speed for the loading stage. The experimental results are gathered in Table 1.

σ [MPa]	$\dot{\varepsilon}_{min}$ [s^{-1}]	Time to failure [s]
37	9.76 10^{-09}	Test interrupted before failure
51	3.36 10^{-08}	Test interrupted before failure
61	7.10 10^{-08}	Test interrupted before failure
65	1.49 10^{-07}	Test interrupted before failure
71	3.56 10^{-07}	289,000
76	2.86 10^{-06}	87,700
79	2.02 10^{-05}	10,500
80	2.34 10^{-05}	4,700
82	6.28 10^{-05}	1,300

Table 1. Experimental data for creep tests on smooth round bars

A typical experimental creep strain history, corresponding to a loading stress of 76MPa and representative of all the creep tests performed on smooth specimens is shown in Fig.4. The creep strain, defined as $\Delta L/L_{0creep}$ during the creep test, is obtained by subtracting the initial strain due to the loading step. In Fig.4a, three creep stages can be identified:

- Primary creep stage where the creep strain rate continuously decreases;
- Secondary creep stage with a nearly constant creep strain rate which is also the minimal creep strain rate;
- Tertiary creep stage where the creep strain rate increases. Fracture occurs at the end of this stage.
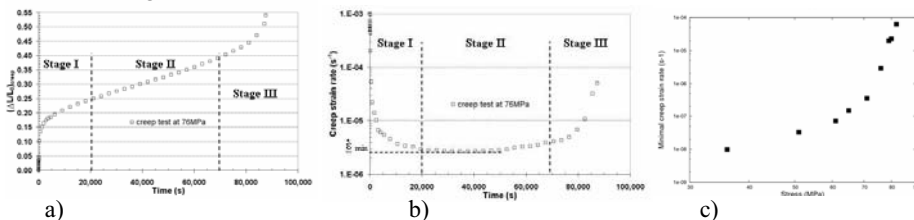

Fig.4. a) Creep strain versus time for a smooth specimen with σ = 76 MPa – b) Creep strain rate versus time a smooth specimen with σ = 76 MPa – c) Creep strain rate versus applied stress

For each creep test, stabilized creep has been observed. Attention is paid to this stationary stage where a minimal creep strain rate is determined. To this end, for each applied stress, the history of the creep strain rate (defined as $\Delta L/L_{0creep}$) divided by the corresponding experimental Δt, is plotted as shown in Fig.4b. The results are given in Table 1 and illustrated in Fig.4c where it can be depicted that experimental points are not linear in a fully logarithmic diagram.

Creep tests on cracked bars

These tests are carried out with the same procedure as on smooth specimens. Crack opening displacement (COD) is measured in order to determinate the minimal COD rate observed in the stationary stage. The experimental results are gathered in Table 2.

σ [MPa]	Minimal COD rate [mm.s^{-1}]	Time to failure [s]
71.8	6.84 10^{-08}	1,578,600
72.7	3.94 10^{-07}	504,000
73.3	2.55 10^{-07}	328,800
74.0	3.08 10^{-07}	331,200
75.2	8.89 10^{-07}	226,200
75.5	4.30 10^{-07}	454,800
78.2	1.41 10^{-06}	100,200
80.1	8.89 10^{-06}	10,200
81.7	2.03 10^{-05}	5,685
81.8	2.46 10^{-05}	4,990
85.	9.57 10^{-05}	1,180
95.2	9.48 10^{-04}	155

Table 2. Experimental data for creep tests on cracked round bars

Creep tests on notched bars

In order to check the sensitivity of the creep time to failure, creep tests on notched round bars were performed. Three notch radii were machined on specimens: 0.8 mm, 1.6mm and 4mm. All notched round bars have the same minimal section radius of b = 2mm (Fig. 5). In the following, the net stress is defined as the load divided by the initial minimal cross section. Reducing the notch radius results in increasing the stress triaxiality ratio τ defined as follows:

$$\tau = \frac{1}{3} + \ln\left(1 + \frac{b}{2r_0}\right). \tag{1}$$

where r_0 is the initial notch radius. Note that r_0 value is 0.45mm for cracked bars.

Notch opening displacement is measured during the creep test. This allows the minimal notched opening displacement rate in the stationary stage to be determined. The experimental results are gathered in Table 3.
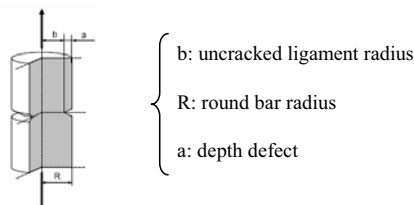
Fig.5. Notched and cracked geometry

b: uncracked ligament radius

R: round bar radius

a: depth defect

Radius of notches (mm)	σ (MPa)	Minimal COD rate (mm.s^{-1})	Time to failure (s)
0.8	70.	1.75 10^{-06}	206,000
0.8	74.	1.47 10^{-05}	33,660
0.8	77.8	5.84 10^{-05}	8,130
1.6	66.4	1.19 10^{-06}	614,000
1.6	70.	1.69 10^{-06}	267,000
1.6	72.1	1.39 10^{-05}	54,930
1.6	73.8	2.81 10^{-05}	21,520
1.6	76.6	2.61 10^{-05}	20,190
1.6	78.	2.58 10^{-04}	2,400
4.	66.5	5.66 10^{-07}	1,397,000
4.	70.2	7.41 10^{-07}	916,800
4.	74.1	2.30 10^{-06}	292,900
4.	74.5	5.51 10^{-06}	178,300
4.	77.7	7.89 10^{-04}	1,520

Table 3. Experimental data for creep tests on notched round bars

Fig.6 plots the time to failure against the stress triaxiality ratio parameterized by the net stress. It can be observed that for a given net stress, by continuously increasing τ, the time to failure first decreases, reaches a minimum value and increases. This peculiar effect seems to indicate that cracked round bars fail later than notched ones.
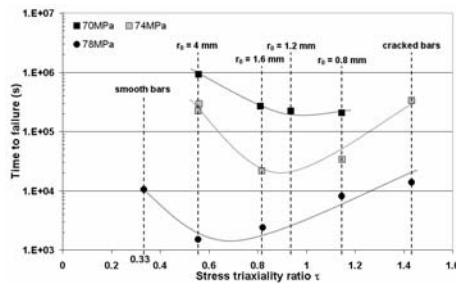

Fig.6. Time to failure versus stress triaxiality ratio parameterized by net stress

Global approach of fracture mechanics for creeping solids

Creep laws

Dealing with primary and secondary creep stages, Eq.(2,3) respectively give the expression the analytical modelling of the creep laws.

Due to the non linearity of the creep strain rates versus nominal stress (Fig.4c) two sets of material parameters gathered in Table 4 are necessary to fit all the creep tests. Typically, the secondary creep stress exponent is required to the following calculation of C* values.

$$\varepsilon = B_1 t^{p_1} \sigma^{n_1} . \tag{2}$$

$$\dot{\varepsilon} = B_2 \sigma^{n_2} . \tag{3}$$

where B_1, p_1, n_1, B_2 and n_2 are parameters of creep law.

Creep law parameters	Low stress	High stress
p_1	$2.63 \ 10^{-01}$	$2.37 \ 10^{-01}$
B_1	$5.07 \ 10^{-10}$	$4.07 \ 10^{-20}$
n_1	3.90	9.45
B_2	$7.06 \ 10^{-16}$	$7.82 \ 10^{-75}$
n_2	4.53	36.5

Table 4. Sets of parameters gathered for creep laws

Load parameters

For each test the load parameter C^* recommended by the NLFM can be estimated [3,4]. For FCNT specimens, C^* can be calculated by Eq.4:

$$C^* = \left(\frac{n_2 - 1}{n_2 + 1}\right) \frac{N_1 \dot{\delta}}{2\pi b^2} . \tag{4}$$

where n_2 is the parameter of the creep law for secondary creep stage (Eq.3), N_1 the load, $\dot{\delta}$ the minimal COD rate and b the uncracked ligament radius (Fig.5).

In Eq.4, $\dot{\delta}$ is the measured COD rate during the creep tests. For engineering components where this variable cannot be accessed, a methodology allowing the calculation of C^* is required. In reference [1], a simplified C^*, noted C_s^*, is proposed, whose expression is displayed in Eq.5. Conceptually, C_s^* is a load parameter devoted to predictive purposes.

$$C_s^* = J_{el}\left[\frac{E\dot{\varepsilon}_{ref}}{\sigma_{ref}}\right] . \tag{5}$$

$$\sigma_{ref} = \frac{N_1}{\pi R b} \quad \text{if } \frac{b}{R} \geq 0,35 . \tag{6}$$

where J_{el} is the elastic evolution of J-integral, E the Young's modulus, $\dot{\varepsilon}_{ref}$ the strain rate associated to the reference stress σ_{ref} given by Eq.6.

All reference stress values are less than 50MPa. Therefore, low stress exponent $n_2 = 4.53$ was selected the calculation of the load parameter C^*.

Master curve

By using first Eq.4, one can plot C^* versus time to failure in order to find a correlation between both parameters. Fig.8 illustrates this correlation, issued from what is commonly called the master curve.
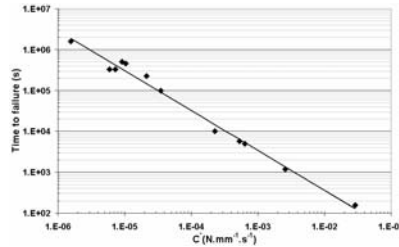
Fig.8. C^* versus time to failure for tests on cracked round bars

A good correlation is clearly established in Fig.8. This C^*-t_R correlation that can be expressed as:

$$t_R \cdot C^{*\,\alpha} = A \,. \tag{7}$$

where α and A are material parameters.

It is to be noted that the knowledge of this master curve allows assessing the lifetime of PA6 cracked bodies.

In order to check the influence of the notch radius on the master curve, results on notched specimens were superimposed with those of cracked ones in Fig.9a. It can then be observed that times to failure of notched specimens overestimate the correlation depicted in Eq.7. In Fig.9a, it seems that cracked specimens give an overconservative prediction of time to failure, by opposition to what was invoked in Fig.6. In Fig.9b, only experimental points of Fig.6 are plotted. One can then follow the trajectory of experimental points for a given net stress value. For instance, at 74MPa, dotted line drawn among open square symbols represents this trajectory. Arrows indicate how the points evolve by decreasing the stress triaxiality ratio. It has to be mentioned that the stress triaxiality ratio can be distinguished here since the C^* formulation directly integrates the experimental COD rate.
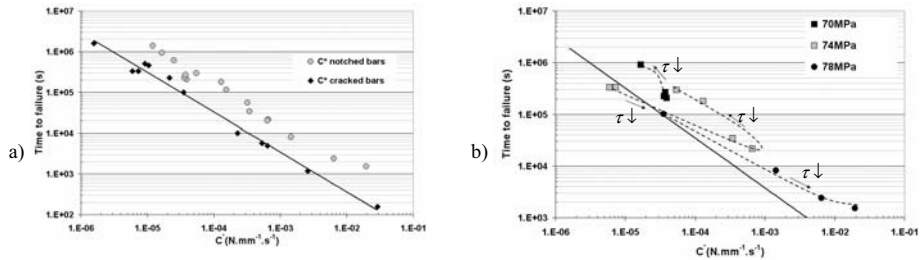

Fig. 9. a) C^* versus time to failure for notched and cracked tests – b) Influence of notch radius on C^* versus time to failure parameterized by net stress

To go further, Fig.10a is plotted by merging C_s^* into the master curve. There is a great discrepancy between C^* and C_s^* values. It can be explained by evaluating the ratio between the two parameters (Eq. 8)

$$\frac{C^*}{C_S^*} \propto \frac{R}{ab} \frac{\dot{\delta}}{\dot{\varepsilon}_{ref}} \,. \tag{8}$$

The same correlation would be obtained if $\dot{\delta}/\dot{\epsilon}_{ref}$ is constant. But by plotting this ratio versus net stresses, it is clearly shown that it depends on the stress level
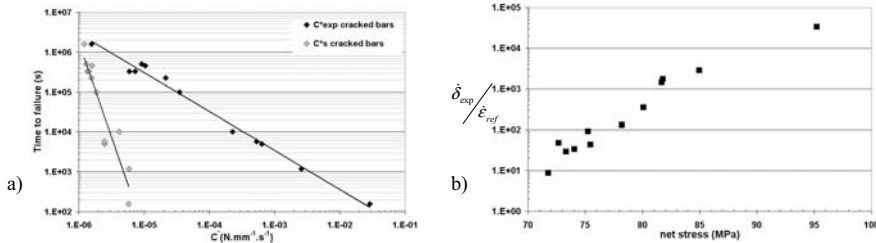

Fig.10. a) C^* and C_s^* versus time to failure for tests on cracked and notched round bars –
b) ($\dot{\delta}_{exp}/\dot{\epsilon}_{ref}$) evolution with net stress

This raises the problem of analytical modeling of the COD rate. It has been shown here that the COD rate corresponding to C_s^* formulation is badly estimated. This underlines the necessity of using Finite Element (FE) analysis. Numerical C^* values can be computed and the strain and stress states within notched and cracked specimens would be better estimated.

Conclusion

The material of interest is a semi-crystalline PA6 that is generally subjected to steady loads. Experimental database has been constituted in order to apply the fracture mechanics of creeping solids concepts. Creep tests were carried out on smooth, notched and cracked round bars. From these experimental data, material parameters of the creep laws were determined. Creep crack test results were utilized to draw the master curve. To do this, experimental C^* was introduced, integrating the measured COD rate. For the sake of prediction, an alternative methodology to calculate C^* was presented, yielding simplified C_s^* parameter. Notched round bar test results were also compared with those of cracked specimens in the master curve. It was then shown that C_s^* values fail to take the stress triaxiality ratio effects. This underlines the necessity of using FE code.

References

[1] AFCEN: *RCC-MR*. Tome 1, Volume Z, Annexe A16 (2007), p. 50-54; 71-72.

[2] R. Piques, E. Molinié, A. Pineau: *Creep and creep-fatigue cracking behaviour of two structural steels*, edited by Elsevier, volume 153 of Nuclear Engineering and Design (1995), p. 223-233.

[3] H. Riedel: *Creep deformation at crack tips in elastic-viscoplastic solids*, Volume 29 of Journal of the mechanics and physics of solids (1981), p. 35-49.

[4] H. Riedel, J.R. Rice: *Tensile cracks in creeping solids*, in: Fracture mechanics, 12th Conference, edited by PC Paris. ASTM STP 700 (1980), p.112-130.

[5] H. Ben Hadj Hamouda, L. Laiarinandrasana, R. Piques: *Fracture mechanics global approach concepts applied to creep slow crack growth in a medium density polyethylene (MDPE)*, Engineering Fracture Mechanics, Issue 14 (2007), p. 2187-2204.